# Macroecology Differentiation Between Bacteria and Fungi in Topsoil Across the United States

Liyuan He, Nicolas Viovy, Xiaofeng Xu

Global Biogeochemical Cycles®

AGU ADVANCING EARTH AND SPACE SCIENCES

RESEARCH ARTICLE
10.1029/2023GB007706

# Macroecology Differentiation Between Bacteria and Fungi in Topsoil Across the United States

**Liyuan He**[1], **Nicolas Viovy**[2], **and Xiaofeng Xu**[1]

[1]Department of Biology, San Diego State University, San Diego, CA, USA, [2]LSCE—Laboratoire des Sciences du Climat et de l'Environnement, Institut Pierre Simon Laplace, Gif-Sur-Yvette, France

**Key Points:**

- We investigated the macroecology of biomass carbon and turnover for fungi and bacteria in natural ecosystems across the United States
- Fungi show stronger biogeographic patterns in biomass carbon than bacteria
- Edaphic properties dominate fungal necromass formation, while mean annual temperature controls bacterial necromass formation across sites

**Supporting Information:**

Supporting Information may be found in the online version of this article.

**Correspondence to:**

X. Xu,
xxu@sdsu.edu

**Citation:**

He, L., Viovy, N., & Xu, X. (2023). Macroecology differentiation between bacteria and fungi in topsoil across the United States. *Global Biogeochemical Cycles*, *37*, e2023GB007706. https://doi.org/10.1029/2023GB007706

Received 23 JAN 2023
Accepted 7 OCT 2023

**Author Contributions:**

**Conceptualization:** Xiaofeng Xu
**Data curation:** Liyuan He, Nicolas Viovy
**Formal analysis:** Liyuan He
**Funding acquisition:** Xiaofeng Xu
**Methodology:** Liyuan He
**Project Administration:** Xiaofeng Xu
**Resources:** Xiaofeng Xu
**Software:** Liyuan He, Xiaofeng Xu
**Supervision:** Xiaofeng Xu
**Visualization:** Liyuan He
**Writing – original draft:** Liyuan He
**Writing – review & editing:** Liyuan He, Nicolas Viovy, Xiaofeng Xu



**Abstract** Bacteria and fungi possess distinct physiological traits. Their macroecology is vital for ecosystem functioning such as carbon cycling. However, bacterial and fungal biogeography and underlying mechanisms remain elusive. In this study, we investigated bacterial versus fungal macroecology by integrating a microbial-explicit model—CLM-Microbe—with measured fungal (FBC) and bacterial biomass carbon (BBC) from 34 NEON sites. The distribution of FBC, BBC, and FBC: BBC (F:B) ratio was well simulated across sites, with variations in 99% ($P < 0.001$), 97% ($P < 0.001$), and 99% ($P < 0.001$) being explained by the CLM-Microbe model, respectively. We found stronger biogeographic patterns of FBC relative to BBC across the United States. Fungal and bacterial turnover rates showed similar trends along latitude. However, latitudinal trends of their component fluxes (carbon assimilation, respiration, and necromass production) were distinct between bacteria and fungi, with those latitudinal trends following inverse unimodal patterns for fungi and showing exponential declining responses for bacteria. Carbon assimilation was dominated by vegetation productivity, and respiration was dominated by mean annual temperature for bacteria and fungi. The dominant factor for their necromass production differs, with edaphic factors controlling fungal and mean annual temperature controlling bacterial processes. The understanding of fungal and bacterial macroecology is an important step toward linking microbial metabolism and soil biogeochemical processes. Distinct fungal and bacterial macroecology contributes to the microbial ecology, particularly on microbial community structure and its association with ecosystem carbon cycling across space.

## 1. Introduction

Soil microbes are the fundamental engine for terrestrial carbon (C) and nutrient cycles (Crowther et al., 2019; Marumoto et al., 1982; Schimel & Schaeffer, 2012; Xu et al., 2013). The biogeography of soil microbes thus has profound significance on C and nutrient dynamics and ecosystem functioning over space (Martiny et al., 2006; Xu et al., 2020). Although the significance of soil microbes in global C and nutrient cycling has been acknowledged, the macroecology of soil microbes is still in its infancy (Xu et al., 2020). Microbial groups such as fungi and bacteria (contributing >90% of soil microbial biomass) are distinct in physiological traits (Kaisermann et al., 2015; Rousk & Bååth, 2007a; Rousk et al., 2009, 2010b). Fungal and bacterial biomass and their turnover rate (mathematical inverse of residence time) have important implications on soil biogeochemistry and, thus, climate projection (Sokol et al., 2022). Consequently, the knowledge of bacterial and fungal macroecology is critically valuable for reducing uncertainties in climate and soil C storage predictions.

Both fungi and bacteria play an essential role in soil processes, including the degradation of soil organic substances (e.g., lignin and cellulose), stabilization of soil organic matter (SOM; e.g., necromass accumulation), and nutrient availability (e.g., mineralization and immobilization) (Liang & Balser, 2011; Lipson et al., 1999; Marumoto et al., 1982; Schimel & Schaeffer, 2012; Sparling, 1997). However, bacterial and fungal communities are different in a multitude of functions such as enzyme production, C assimilation, respiration, nutrient uptake, and thus the C sequestration potential (Bailey et al., 2002; Boer et al., 2005; Van Der Heijden et al., 2008). In addition, studies suggested distinct preferences of fungi and bacteria on soil pH, soil moisture, oxygen concentration, and nutrient concentration (Drenovsky et al., 2004; Högberg et al., 2007; Kaisermann et al., 2015; Rousk et al., 2010b). For example, a study reported a strong bacterial dependence on soil pH, but a weak correlation of fungi with soil pH in cropland soils (Rousk et al., 2010a). Therefore, capturing variations in the relative abundance of fungi and bacteria and their controlling factors can help improve C and nutrient cycling predictions.

Regional observational networks have been implemented to investigate the ecosystem structure and function across space, thus fulfilling the goal of advancing microbial macroecology. National Ecological Observatory Network (NEON) provides large-scale measurements using standardized protocols across spatial and temporal scales, which is particularly valuable for microbial variables varying over >3 orders of magnitude and usually measured using various approaches (Kampe et al., 2010; Keller et al., 2008). Although these measurements allow the community to investigate the distribution of soil microbes on a large scale (Keller et al., 2008), a mechanistic understanding of microbial macroecology is still lacking. The microbial-explicit models, incorporating detailed descriptions of biological metabolism and nutrient cycling, potentially advance our understanding of the microbial biogeography (Flato, 2011; Haefner, 2005). Incorporating microbial roles in the community land model (CLM), the CLM-Microbe model considers the physiological processes of fungi and bacteria and their controls on soil organic material decomposition processes (He, Lai, et al., 2021, He, Lipson, et al., 2021). Consequently, integrating NEON observational data with the CLM-Microbe model offers an opportunity to compare the macroecology of fungi and bacteria.

To investigate the macroecology of fungal and bacterial biomass and turnover, we integrated in situ observations of fungal (FBC) and bacterial (BBC) biomass C derived from the phospholipid fatty acid (PLFA) measurements with the CLM-Microbe model at 34 NEON sites. This study aimed to understand the biogeographic patterns of fungal and bacterial biomass C and turnover and their underlying mechanisms. We first calibrated the CLM-Microbe model simulation against the observed FBC, BBC, FBC:BBC (F:B) ratio for 34 NEON sites. Secondly, we investigated the biogeographic patterns of FBC, BBC, and F:B ratio and identified their controls based on Bray-Curtis dissimilarity matrices of FBC, BBC, and F:B ratio and Euclidean distance of environmental factors. Finally, we integrated the knowledge of spatial patterns of fungal and bacterial biomass C turnover rates to develop a framework depicting their underlying mechanisms given microbial C assimilation, respiration, and lysis.

## 2. Methods and Materials

### 2.1. Study Area

The United States has a large variability in vegetation, landforms, climate, and ecosystem performance. To capture the environmental variations in the study area, NEON has partitioned the United States, including the continental United States, Alaska, Hawaii, and Puerto Rico, into 20 eco-climatic domains using a statistical analysis of multivariate geographic clustering based on nine ecoclimatic state variables such as total precipitation in growing and nongrowing seasons and total solar insolation in growing and nongrowing seasons (Hargrove & Hoffman, 2004). Collectively, domains ensure the capability of NEON sites to represent the environmental variability in the United States. In each domain, one core site for the representativeness of the environment (fixed for 30 years) and two relocatable sites (changed every 5–10 years) were implemented (Keller et al., 2008). Taken together, 47 terrestrial field sites were strategically instrumented across 20 ecoclimatic domains in the United States, providing a crucial basis for understanding regional- and continental-scale ecological processes and monitoring and predicting environmental change (Kao et al., 2012; Metzger et al., 2019).

### 2.2. Fungal and Bacterial Biomass Data and Site Selection

The Soil Microbe Biomass data set (NEON data products: DP1.10104.001) provides quantitative microbial biomass estimates in soil samples (National Ecological Observatory, 2021a). Microbial biomass is measured by phospholipid fatty acid (PLFA) analysis, which is widely considered to be a reliable (Zelles, 1999) and sensitive (Allison & Martiny, 2008) proxy of the soil microbial community (Zhang et al., 2019). Sample collection and PLFA measurement were performed using standardized operating procedures across sites. Briefly, soil sampling occurs annually at least one site in each domain and once (sites with short growing seasons) to three times (sites with long growing seasons) per year, with collections occurring at every sampled site during the historic peak in vegetation greenness. The NEON samples were collected for the top 30 cm soil, with organic and mineral soils sampled separately. Soil samples were homogenized, removed from coarse compartments, frozen, and shipped to an analytical facility on dry ice. Microbial lipid biomarkers were then extracted and quantified using either Gas Chromatography-Mass Spectrometry (2018 and earlier) or Gas Chromatography (2019 and later) (Buyer & Sasser, 2012; Gomez et al., 2014). The archived data set can provide reliable estimates of individual microbial

lipids and total measured phospholipids in each sample. The microbial biomass data set used in this study was downloaded from https://data.neonscience.org/data-products/DP1.10104.001 on 21 May 2021.

Individual lipids were used as biomarkers to indicate broad groups within the microbial community. 18:2 ω6,9c (NEON publication name: cis18To2n912Concentration) for general fungi and c14:0, c15:0, c16:0, c17:0, and c18:0 (corresponding to c14To0Concentration, c15To0Concentration, c16To0Concentration, c17To0Concentration, and c18To0Concentration of NEON publication name, respectively) for general bacteria (Willers et al., 2015; Zelles, 1997). Fungal and bacterial fatty acids were converted into biomass C using the following factors: bacterial biomass 363.6 nmol PLFA = 1 mg C (Frostegård & Bååth, 1996), and fungal biomass 11.8 nmol PLFA = 1 mg C (Klamer & Bååth, 2004). Since this study focused on the spatial pattern of fungal and bacterial distribution, FBC and BBC were calculated as the average of multiple samplings (i.e., different plots and sampling dates) for each site.

The microbial biomass data set provided data for 40 terrestrial sites in 20 ecoclimatic domains (Figure S2 and Table S2 in Supporting Information S1). Given the effects of disturbance on the soil microbial community and lack of validation of such effects in the CLM-Microbe model, five sites with disturbance or land management practices, that is, cropland (site ID: JERC, KONA, LAJA, and STER) and pasture (site ID: DSNY) sites, were excluded. Soil microbial biomass C accounts for a relatively small proportion (0.9%–6.5%) of SOC (Xu et al., 2013). After comparing the ratio of microbial biomass C to SOC, microbial biomass C contributed disproportionately high to SOC (18%) at one site of the tundra domain (TOOL). Therefore, TOOL was excluded from the data set. Finally, 34 sites (18 cores and 16 relocatable sites) with observed data spanning various sampling years (2017–2020) and durations (1–4 years) were included for model calibration and further analysis (Figure S1 and Table S2 in Supporting Information S1). Such sites are distributed in 19 ecoclimatic domains along gradients of latitude (18–65°N), mean annual temperature (MAT; −2–25°C), and mean annual precipitation (MAP; 200–2,680 mm). Correspondingly, multiple vegetation types, that is, deciduous forest, evergreen forest, wetland, mixed forest, grassland, and shrub, were found across sites (Table S2 in Supporting Information S1).

### 2.3. Soil Physiochemical Data

We used NEON soil physical and chemical properties, megapit data set (NEON data products: DP1.10096.001) to represent soil properties (National Ecological Observatory, 2021b). We obtained the variables of soil clay (NEON fieldname: clayTotal), silt (siltTotal), sand (sandTotal), bulk density (bulkDensExclCoarseFrag), soil pH measured in water (phH2o), soil organic C (estimatedOC; SOC), and total nitrogen (nitrogenTot; TN) for <2 mm soil fraction from such a data set. Soil samples for physiochemical properties were sampled by soil layer, with organic and mineral soils sampled separately. To estimate the soil physiochemical properties in the top 30 cm, the top and bottom depths of each soil layer were used to define soil layer depths along the soil profile. Only measurements within 0–30 cm depth were selected, then the soil property was averaged using horizon thickness as weights. For soil horizons with bottom depth >30 cm, only segments within 0–30 cm were used for calculation, assuming that soil property in the soil horizon was uniform. Some soil layers with unmeasurable layer traits (e.g., missing bulk density measurements) were excluded from estimation. Therefore, bulk density belonging to regular sample type within 0–30 cm was finally adopted for converting mass-based soil physiochemical properties to area-based ones such as SOC and TN.

### 2.4. Model Representation of Fungal and Bacterial Biomass

The CLM-Microbe model was built on the model framework developed by Xu et al. (2014) and the default CLM4.5 (Koven et al., 2013). It has been coupled with a microbial functional group–based methane module (Wang et al., 2019; Xu et al., 2015) and applied to quantify the fungal and bacterial biomass dynamics in natural ecosystems (He, Lipson, et al., 2021). The CLM4.5 classifies litter into three pools, that is, litter 1 (labile), litter 2 (cellulose), and litter 3 (lignin), and soil organic matter (SOM), materials left during later stages of organic C decay, into four pools, that is, SOM 1, SOM 2, SOM 3, and SOM 4 (low-high recalcitrance). The three litter pools and four SOM pools differ in base decomposition rate, with the turnover times of litter pools ranging from 20 hr to 71 days and that of SOM pools ranging from 14 days to 27 years (Figure S1 in Supporting Information S1). Coarse woody debris (CWD) is fragmented, decomposed, and gradually transferred into litter pools and from litter to SOM pools (Koven et al., 2013; Thornton et al., 2007). In addition to eight C pools (three litter, four

SOM, and CWD pools) in the default CLM4.5, we introduced dissolved organic matter (DOM) and fungal and bacterial biomass pools in the CLM-Microbe model. The model version used in this study has been archived as (Xu et al., 2022).

In the CLM-Microbe model, fungal and bacterial biomass is the balance of C input from the decomposition of SOM, DOM, and litter and C loss through microbial lysis and respiration. Specifically, fungi and bacteria receive C through the transitions from litter, DOM, and SOM pools; fungi and bacteria lose C through the transitions from fungal and bacterial biomass pools to DOM and SOM pools and the atmosphere. The conceptual diagram of the CLM-Microbe model and major parameters were compiled and displayed in Figure S1 and Table S1 in Supporting Information S1.

The decompositions of SOM, DOM, and litter are controlled by their potential decomposition rates and environmental conditions. The decomposition processes in the CLM-Microbe model are defined following the equations given below,

$$D_C = k \times r_{\text{depth}} \times r_{t\text{soil}} \times r_{\text{water}} \times r_{O_2} \tag{1}$$

$$r_{\text{depth}} = \exp\left(-\frac{z}{z_\tau}\right) \tag{2}$$

$$r_{t\text{soil}} = Q_{10}^{\frac{T_{\text{soil},j} - T_{\text{ref}}}{10}} \tag{3}$$

$$r_{\text{water}} = \begin{cases} 0 & \text{for } \varphi_j < \varphi_{\min} \\ \frac{\log(\varphi_{\max}/\varphi_j)}{\log(\varphi_{\max}/\varphi_{\min})} & \text{for } \varphi_{\min} \le \varphi_j \le \varphi_{\max} \\ 1 & \text{for } \varphi_j > \varphi_{\max} \end{cases} \tag{4}$$

$$r_{O_2} = f_r \times (1 - f_{\text{inun}}) \times \max(O_{2\text{unsat}}, O_{2\min}) + f_{\text{inun}} \times \max(O_{2\text{sat}}, O_{2\min}) \tag{5}$$

where $D_C$ is the rate of substrate (e.g., SOM, DOM, and litter) breakdown; $k$ is the potential decomposition rate; $r_{O_2}$ represents the environmental modifier determined by soil oxygen concentration; $r_{\text{depth}}$ is the environmental modifier determined by soil depth; $r_{\text{water}}$ is environmental modifier determined by soil moisture; $r_{t\text{soil}}$ means the environmental modifier determined by soil temperature; $z$ means soil depth; $z_\tau$ is the e-folding depth for decomposition; $T_{\text{soil},j}$ is soil temperature at layer $j$; $T_{\text{ref}}$ is the reference temperature for decomposition, which is set as 25°C; $Q_{10}$ indicates the temperature dependence of decomposition, it is the ratio of the rate at a specific temperature to that at 10°C lower; $\varphi_j$ is the soil water potential in layer $j$; $\varphi_{\min}$ is a lower limit for soil water potential control on decomposition rate (set to −10 MPa), $r_{\text{water}}$ will be set as 0 if $\varphi_j$ is lower than $\varphi_{\min}$; $\varphi_{\max}$ is the upper limit for soil water potential control on decomposition, which equals to the saturated soil matric potential, $r_{\text{water}}$ will be set as 1 if $\varphi_j$ is higher than $\varphi_{\max}$; $w_{\text{soil},j}$ means soil water content in layer $j$; $f_r$ is the rooting fraction by soil depth; $f_{\text{inun}}$ means the fraction of inundated area; $O_{2\text{unsat}}$ represents the oxygen available to that demanded by roots and aerobic microbes in unsaturated area; $O_{2\min}$ denotes the ratio between minimum anaerobic decomposition rate and potential aerobic decomposition rate in soil (set to 0.2); $O_{2\text{sat}}$ represents the oxygen available to that demanded by roots and aerobic microbes in saturated area; $r_{O_2}$ will be set as 1 in oxic conditions, while it will be estimated as the weighted average of oxygen stress in saturated and unsaturated areas in anoxic conditions.

Carbon use efficiency (CUE) of soil microbes for assimilating three litter pools in the CLM-Microbe model is determined following the equation in Sinsabaugh et al. (2013). In addition, CUE is reported to vary with temperature, showing a coefficient of −0.012 with increasing temperature (Devêvre & Horwáth, 2000; Xu et al., 2014). Therefore, we assumed that CUE decreased compared with the ambient thermal regime of microbes' habitats following the equation below:

$$\text{CUE} = (\text{CUE}_{\max} - \text{CUE}_T \times (T - T_{\text{CUEref}})) \times (M_{\text{C:N}}/S_{\text{C:N}})^{0.6} \tag{6}$$

where CUE is C use efficiency, which is defined as the growth to assimilation ratio for soil microbes; $\text{CUE}_{\max}$ is the maximum value of C use efficiency; $\text{CUE}_T$ is the coefficient indicating the dependence of C use efficiency on temperature; $T_{\text{CUEref}}$ is the reference temperature of C use efficiency, which is defined as 15°C in

the CLM-Microbe model; $M_{C:N}$ means the C:N ratio of soil microbial biomass, which is defined as 8 in the CLM-Microbe model; $S_{C:N}$ represents C:N ratio of the substrate (e.g., litter).

The C flow from litter and SOM pools to soil microbes is partitioned by fungal and bacterial biomass pools based on the C:N ratio of fungal and bacterial biomass. The fraction factor quantifying bacteria C gain from litter and SOM is calculated independently for each substrate, which is based on the weighted average of assimilation efficiency of fungi and bacteria following the equation below,

$$fb = \frac{\left(B_{C:N}/S_{C:N}\right)^{0.6}}{\left(F_{C:N}/S_{C:N}\right)^{0.6} + \left(F_{C:N}/S_{C:N}\right)^{0.6}} \quad (7)$$

$$ff = 1 - fb$$

where *fb* is the fraction of C flowing into bacteria; *ff* is the fraction of C flowing into fungi; $B_{C:N}$ means the C:N ratio of BBC; $F_{C:N}$ means the C:N ratio of FBC; $S_{C:N}$ represents the C:N ratio of substrates (e.g., litter and SOM).

Bacterial and fungal growth is susceptible to environmental variations such as soil moisture and temperature. In addition, fungi and bacteria have different turnover times; therefore, different lysis rate constants were adopted for fungi and bacteria in the CLM-Microbe model (He, Lipson, et al., 2021). As a result, in the CLM-Microbe model, the fungal and bacterial biomass lysis is represented as the interactive effects of their lysis rate constants and environmental factors, that is, $r_{O_2}$, $r_{water}$, $r_{tsoil}$, and $r_{depth}$, as described above. Microbial respiration is widely affected by multiple abiotic and biotic factors such as substrate concentration and availability, soil moisture, and soil temperature (Gomez-Casanovas et al., 2012; Zhang et al., 2013). Therefore, in the CLM-Microbe model, fungal and bacterial respiration is represented as the interactive effects of substrates (i.e., DOM, SOM, and litter), environmental factors (i.e., $r_{O_2}$, $r_{water}$, and $r_{tsoil}$), and fraction factors quantifying C being respired by fungi and bacteria in transitions (Table S1 in Supporting Information S1).

### 2.5. Model Forcing Data

The forcing data for the CLM-Microbe model include meteorological variables such as air temperature, relative humidity, incoming solar radiation, longwave radiation, precipitation rate, surface pressure, and surface winds. Although those variables are available from multiple sources such as eddy covariance tower measurements and a wide array of global data sets, few data sets covered the sampling years of NEON measurements.

Given that the sampling years of sites span from 2017 to 2020, we chose the CRUNCEP v9 data set to force the CLM-Microbe model as it has been widely used to force the community land model. The CRUNCEP is a combination of two existing data sets, that is, the Climate Research Center time-series data set of 0.5° × 0.5° at a monthly scale and the National Centers for Environmental Prediction reanalysis data set of 2.5° × 2.5° at a 6-hourly scale. The CRUNCEP v9 data set provides 6-hourly data of meteorological variables with a spatial resolution of 0.5° × 0.5° spanning from 1901 to 2020. Finally, we extracted the forcing data from 1 January 1981 through 31 December 2020 from the CRUNCEP v9 data set using each study site's latitude and longitude information (Table S2 in Supporting Information S1).

Since the standard model forcing data for single-point simulations are in the half-hourly time steps, the extracted 6-hourly data for each study site were interpolated to half-hourly steps with multiple approaches. Specifically, the incoming solar radiation was interpolated using the cosine algorithm with approx.cos; the precipitation rate was interpolated using nearest-neighbor interpolation via interp1; whereas air temperature, relative humidity, longwave radiation, surface pressure, and surface wind were linearly interpolated via the na.approx function in R (R for Mac OS X version 3.5.3).

### 2.6. Model Implementation

The model implementation was carried out in three stages. First, we ran the accelerated decomposition spin-up to allow the system to reach its steady-state (Koven et al., 2013; Thornton & Rosenbloom, 2005). Due to the differences in the length of time to reach a steady state among biomes, we set the model simulations as 1,500 years for tropical and temperate biomes (i.e., sites located outside the Taiga domain or not considered as wetlands), 2000 years for boreal and Arctic biomes (i.e., sites in the Taiga domain), and 3,000 years for wetlands (i.e., sites

dominated by wetlands). Then, we ran a final spin-up of 100 years to ensure the system was ready for transient simulations during 1850–2020. The CLM-Microbe model was parameterized by biome (He, Lipson, et al., 2021); we thus classified the sites into biomes by their most dominant land cover types and their domain features, that is, boreal forests (BONA and DEJU), wetlands (WOOD and OSBS), grassland (CPER, OAES, DCFS, and NOGP), temperate broadleaf forests (BLAN, CLBJ, GRSM, HARV, KONZ, LENO, MLBS, ORNL, SCBI, STEI, TALL, TREE, UKFS, and UNDE), temperate coniferous forests (DELA, JORN, MOAB, NIWO, ONAQ, RMNP, SJER, SOAP, WREF, and YELL), and tropical/subtropical forests (GUAN and PUUM). The initial setting for microbial parameters was adopted from He, Lipson, et al. (2021), with the same parameter set for sites in the same biome.

To produce realistic soil and vegetation conditions in the CLM-Microbe model for each site, we extracted the SOC of the top 30 cm soil profile from the Harmonized World Soil Database (HWSD, https://daac.ornl.gov/cgi-bin/dsviewer.pl?ds_id=1247) and gross primary productivity (GPP) and net primary productivity (NPP) using the MODIS gridded data set with a spatial resolution of 30 s during 2000–2015 (http://files.ntsg.umt.edu/data/NTSG_Products/) using site latitude and longitude information. Although NEON provided SOC of soil horizons, such measurements are for ≤2 mm soil fraction. The contribution of not fully decomposed plant and microbial detritus to SOC is underestimated. Therefore, if the extracted SOC of the top 30 cm from the HWSD data set were lower than the SOC (≤2 mm) from the NEON soil physical and chemical properties of the megapit data set (NEON data products: DP1.10096.001), we then adopted NEON reported SOC. In addition, if GPP and NPP from the MODIS data set were 100% higher or 50% lower than global averages of each biome (Chapin et al., 2011), we used the reported average of each biome (Chapin et al., 2011; Jobbágy & Jackson, 2000).

Taken together, we optimized the model parameters based on soil and vegetation conditions reported by HWSD and MODIS, respectively, and FBC and BBC based on NEON observations. We primarily focused on the parameters (in italics) related to plant photosynthesis (e.g., *flnr*), and e-folding depth for decomposition (e.g., *decomp_depth_efolding*) to match the reported GPP, NPP, and SOC in the top 30 cm. To calibrate the model to fit the observed FBC and BBC, we adjusted soil microbial parameters related to microbial turnover (*k_fungi* and *k_bacteria*), microbial C assimilation efficiency (*m_rf_s1m*, *m_rf_s2m*, *m_rf_s3m*, and *m_rf_s4m*), and the proportion of C being released as respiration (*m_batm_f* and *m_fatm_f*) to optimize the model simulations of FBC and BBC.

### 2.7. Model Evaluation

To evaluate the model performance in capturing the spatial variation in the fungal and bacterial biomass C distribution, we compared the observed and simulated FBC, BBC, and F:B ratio during corresponding sampling months for each site (Table S2 in Supporting Information S1). Although exact sampling times of NEON sites have been recorded, sampling of subplots was implemented on multiple days, producing multiple sampling dates per plot. We thus compared the simulated and observed data of sampling months during such years for each site instead. The coefficient of determination ($R^2$) was used to evaluate the overall model performance across space. The coefficient of determination ($R^2$) was calculated following the equation below,

$$R^2 = 1 - \frac{\sum_{i=1}^{N} (y_i - \hat{y}_i)^2}{\sum_{i=1}^{N} \left(y_i - \overline{y}\right)^2} \tag{8}$$

where $y_i$ is the observed value; $\hat{y}_i$ represents the simulated value; $\overline{y}$ is the mean of the observed value; $N$ is the number of data points. Higher $R^2$ values indicate better model performance, while lower $R^2$ values mean worse model performance.

### 2.8. Microbial Turnover Estimation

Fungal and bacterial turnover rates were estimated from their C assimilation or microbial respiration and necromass production during sampling years (Figure S1 in Supporting Information S1). In the CLM-Microbe model, fungal and bacterial C assimilation is the C gain from three litter pools (i.e., litter 1, litter 2, and litter 3), four SOM pools (SOM 1, SOM 2, SOM 3, and SOM 4), and a DOM pool allocated to fungal and bacterial biomass

pools, respectively. Fungal and bacterial respiration is the C loss from fungal and bacterial biomass pools during microbial metabolic processes such as decomposition of three litter pools and four SOM pools, respectively. Fungal and bacterial lysis rates were estimated by the C flow from fungal and bacterial biomass pools to the DOM and four SOM pools, respectively. We assumed that microbial C assimilation equaled the sum of microbial respiration and lysis after reaching a steady state. In this study, the turnover rates for fungal and bacterial species were calculated using the sum of fungal and bacterial respiration and lysis rates divided by their biomass C pools, respectively, following the equation below,

$$\tau = \frac{R + L}{B} \tag{9}$$

where $\tau$ is a fungal or bacterial biomass C turnover rate; $R$ means fungal or bacterial respiration rate; $L$ indicates a fungal or bacterial lysis rate; $B$ denotes fungal or bacterial biomass C pool size.

### 2.9. Statistical Analysis

Due to the non-normality of FBC, BBC, and F:B ratio, we performed a 10-base logarithm transformation for robust analysis. To investigate the biogeographic patterns of fungal and bacterial biomass C, we performed simple linear regression analyses to examine relationships of fungal and bacterial biomass C and their ratio with latitude, climatic factors such as MAT and MAP, soil microclimate including soil moisture (SM) and soil temperature (ST) during sampling months, and edaphic properties comprising SOC, total nitrogen (TN), SOC:CN (C:N) ratio, soil pH, bulk density, and soil texture using the lm function in *R*. To estimate binary interactions between representative vegetative (NPP) and edaphic (SM, ST, SOC, TN, Clay, and soil pH) factors on FBC, BBC, F:B ratio, we conducted multiple linear regression analyses using the "lm" function provided in *R* considering the effects of individual factors and interactions between those factors. For the trends of fungal and bacterial biomass C turnover rates, C assimilation, and C loss as microbial respiration and necromass production along the latitude, we conducted simple linear regression analyses using the "lm" function and nonlinear regression with the "nls" function estimated using the least-squares method in *R*. Correlations of FBC, BBC, F:B ratio, fungal and bacteria C assimilation, and C loss as microbial respiration and necromass production with environmental factors were estimated using Pearson's correlation. To identify the critical controls for fungal and bacterial turnover rates, C assimilation, and C loss as microbial respiration and necromass production, we used the "XGBoost" function to infer the relative feature importance in the model. To investigate environmental factors influencing fungal and bacterial biomass C distribution, we used Mantel tests to assess the correlations of fungal and bacterial biomass C matrices with matrices of explanatory variables such as MAP, MAT, labile component of litter (LITR1C), recalcitrant SOC component (SOIL4C), DOM, NPP, SOC, TN, C:N ratio, sand, clay, pH, and bulk density. The dissimilarity matrices of explanatory variables were calculated on the basis of Euclidean distance, while Bray-Curtis distance was used to evaluate dissimilarity matrices of fungal and bacterial biomass C.

We used the Akaike information criterion (AIC) as a model selection criterion. All statistical analyses were performed, and relevant figures were plotted using the "soiltexture" (Moeys, 2018), "linkET" (Huang, 2021), "xgboost" (Chen & He, 2015), "ggplot2" (Wickham & Chang, 2016), and "basicTrendline" (Mei et al., 2018) packages in R version 3.5.3 for Mac OS X (https://www.r-project.org). Figure S2 in Supporting Information S1 was produced with ArcGIS (version 10.6).

## 3. Results and Discussion

### 3.1. Evaluation of Simulated Fungal and Bacterial Biomass C Across Sites

The CLM-Microbe model can reproduce FBC, BBC, and F:B ratio across sites (Figure 1). Specifically, the CLM-Microbe model explained 99%, 97%, and 99% of the variation in FBC, BBC, and F:B ratio, respectively. In addition, the accuracy evaluation using mean absolute error (MAE) and root mean squared error (RMSE) indicated small biases of the CLM-Microbe model in reproducing FBC (MAE = 12.1 g C $m^{-2}$ and RMSE = 25.1 g C $m^{-2}$), BBC (MAE = 1.9 g C $m^{-2}$ and RMSE = 3.2 g C $m^{-2}$), the F:B ratio (MAE = 0.4 and RMSE = 0.7) across sites (Table S3 in Supporting Information S1). Furthermore, we also compared the CLM-Microbe model—simulated microbial respiration with data extracted from a global map of heterotrophic respiration (Warner et al., 2019). Excluding two sites (tropical/subtropical area; because of the large bias and small sample size in that area) from

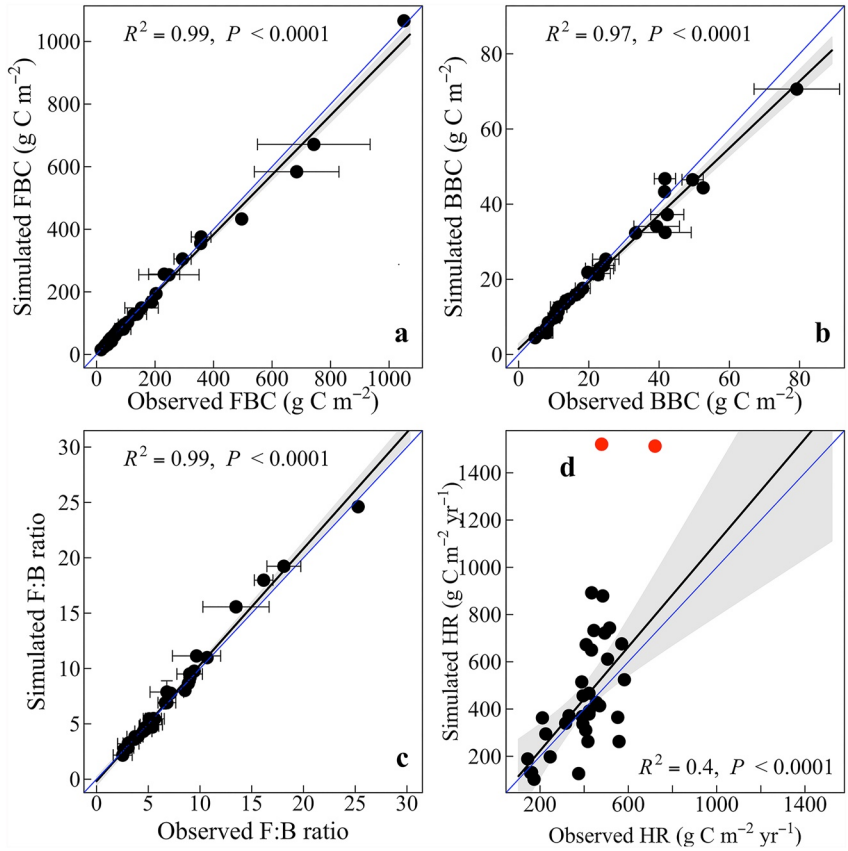


**Figure 1.** Scatterplot for the comparison between observed and the CLM-Microbe simulated microbial biomass C; (a) fungal biomass carbon (FBC), (b) bacterial biomass carbon (BBC), (c) FBC:BBC ratio, and (d) HR. Black solid lines are for the linear regression model between observed and simulated values, while blue solid lines indicate the 1:1 line. Observed heterotrophic respiration data were extracted from a global map (Warner et al., 2019). Two outliers from tropical/subtropical forests marked in red were excluded from the linear regression.

the linear regression, we observed a significant correlation between them (Figure 1d). The high consistency between simulated and observed microbial biomass and community composition can be explained by the explicit representation of soil microbial processes in the model. For example, environmental impacts on microbial C assimilation have been represented by considering the role of soil moisture, temperature, oxygen concentration, and substrate (e.g., dissolved organic matter, SOM, and litter) on microbial C gain in the CLM-Microbe model (Figure S1 in Supporting Information S1). In addition, fungi and bacteria have different turnover rates (Rousk & Bååth, 2011). Correspondingly, parameters representing fungal and bacterial biomass turnover were adopted to signify their differences in biomass turnover rates.

### 3.2. Biogeographic Patterns of Fungal and Bacterial Biomass C

Fungal biomass C was more responsive to environmental variations relative to bacterial biomass C (Figures S3–S8 and Table S4 in Supporting Information S1). For example, linear regression models suggested that FBC exhibited significant reverse unimodal relationships with latitude, unimodal relationships with C:N ratio, positive linear relationships with SOC and TN, and negative linear relationships with MAT, soil pH, and bulk density. In contrast, we failed to observe clear patterns of BBC along latitude, MAT, SOC, TN, and bulk density, but instead found that BBC showed unimodal relationships with C:N ratio and negative linear relationships with soil pH. Consistent with our findings, our previous work also found better modeling fit of latitude, MAT, SOC, C:N ratio, and pH with FBC than with BBC (He et al., 2020). In contrast to the stronger biogeographic patterns of FBC than of BBC in this study, Chen et al. (2015) found that bacterial biomass showed stronger correlations with MAP, MAT, and SOC across 24 arid and semi-arid ecosystem sites compared with fungal biomass. Rousk

et al. (2010a) also observed significant positive effects of soil pH on the abundance of bacteria, but that of fungi was unaffected by pH. The discrepancies among studies can be attributed to five reasons. First, different climates of study regions may cause the distinct responses of fungal and bacterial biomass. Chen et al. (2015) conducted their studies in Mongolia Plateau, arid and semiarid areas, where precipitation is the predominant limiting factor for plant and microbial activities (Harper et al., 2005). As fungi are more tolerant to water stress than bacteria (Manzoni et al., 2012), bacteria may be more constrained by water availability and related abiotic factors due to compounding effects along the precipitation gradient. For example, bacteria tended to be more responsive to the interactions between SM and ST (Table S5 in Supporting Information S1). Second, ecosystem types might be another reason. The NEON sites included in this study are confined to natural ecosystems, while Rousk et al. (2010a) performed the soil sampling in cropland ecosystems. The altered fungal and bacterial community composition due to cultivation activities in croplands relative to wildlands may explain the discrepancy between studies (French et al., 2017). Third, bacteria are more accustomed to local edaphic conditions than fungi. For example, *Pseudomonas* can detect the biological hot spots caused by water flow and shift community structures accordingly to adapt to the local environment (Bundt et al., 2001). To represent biogeographic patterns of fungal and bacterial biomass C, environmental factors in this study are annual averages (MAP, MAT, NPP, SOC, TN, C:N ratio, sand, clay, pH, and bulk density) or averages of sampling months (i.e., SM and ST). Those partially excluded variations (variation within months or years) of microenvironments from this analysis may cause weak bacterial responses to environmental factors. Fourth, the faster turnover rates of bacteria may cause the independence of BBC from environmental factors. BBC has a turnover rate faster than FBC, thus indicating a more prominent variation in biomass maintenance. Large variations in BBC induced by the faster turnover rates of bacteria may weaken the response of BBC to biogeographic factors (Gu et al., 2004). Lastly, the difference in soil sampling depth might also contribute to differences in fungal and bacterial responses to environmental factors among studies. For example, Zhang et al. (2020) did not observe significant biogeographical patterns of fungal and bacterial PLFAs in topsoil (0–10 cm), but they documented significant correlations of fungal PLFAs with aridity index, MAP, MAT, and plant species richness and between bacterial PLFAs and MAP in subsoil (30–50 cm). The sampling depths of 0–30 cm for NEON data but 0–40 cm in Chen et al. (2015) might contribute to the discrepancy between studies.

### 3.3. Macroecology of Fungal and Bacterial Biomass C

The MAT, SOC, recalcitrant SOC component (SOIL4C), and C:N ratio significantly ($P < 0.05$) correlated with both observed and simulated FBC and F:B ratios. In addition, bulk density was significantly correlated with both observed and simulated FBC and observed F:B ratio. Soil pH had a significant correlation with the simulated F:B ratio (Figure 2). The significant controlling effects of MAT, C:N ratio, SOC, soil pH, and bulk density on FBC and F:B ratio agreed with our regression models (Figures S3–S7 and Table S4 in Supporting Information S1). In line with our findings, previous studies confirmed the significant roles of MAT, SOM quality and quantity, pH, and bulk density in shaping the distribution of FBC and F:B ratio (Chen et al., 2015; He et al., 2020; Högberg et al., 2007; Yu et al., 2022). Temperature can influence microbial biomass in multiple ways, for example, altering the rates of substrate uptake and microbial respiration and death and shaping soil microbial biomass along temperature gradients (He & Xu, 2021; Joergensen et al., 1990; Xu et al., 2014). Edaphic properties determine the physical and chemical environment for microbial growth. For example, SOM (represented by SOC and TN), vital energy and nutrient source for microbes, is important in shaping microbial communities (Burns et al., 2016; Drenovsky et al., 2004; Schimel & Schaeffer, 2012; Schnürer et al., 1985). Notably, previous studies found that SOCs, especially the recalcitrant components, favors the dominance of fungi due to the higher capability of fungi in producing enzymes and processing recalcitrant products (Phillips et al., 2014; Talbot et al., 2013). Manipulative experiments also reported significant changes in microbial composition and F:B ratio with amendments of C and nitrogen (Drenovsky et al., 2004; Zhou et al., 2017).

In addition to SOM, other soil properties such as pH and bulk density critically influence the microbial community composition. Soil pH was found to exert direct effects on microbial growth. Rousk et al. (2009) investigated how pH affected the growth of fungi and bacteria and found that bacterial growth significantly increased while fungal growth exponentially decreased along a pH gradient of 4.5–8.3. Soil pH can also indirectly influence microbial growth by altering other co-varying factors such as nutrient and substrate availability (Kemmitt et al., 2006; Waldrop et al., 2017). The variations in soil pH can therefore regulate microbial community dynamics. Bulk density indicates the porosity of soil profiles and further oxygen and moisture availability. Fungi are

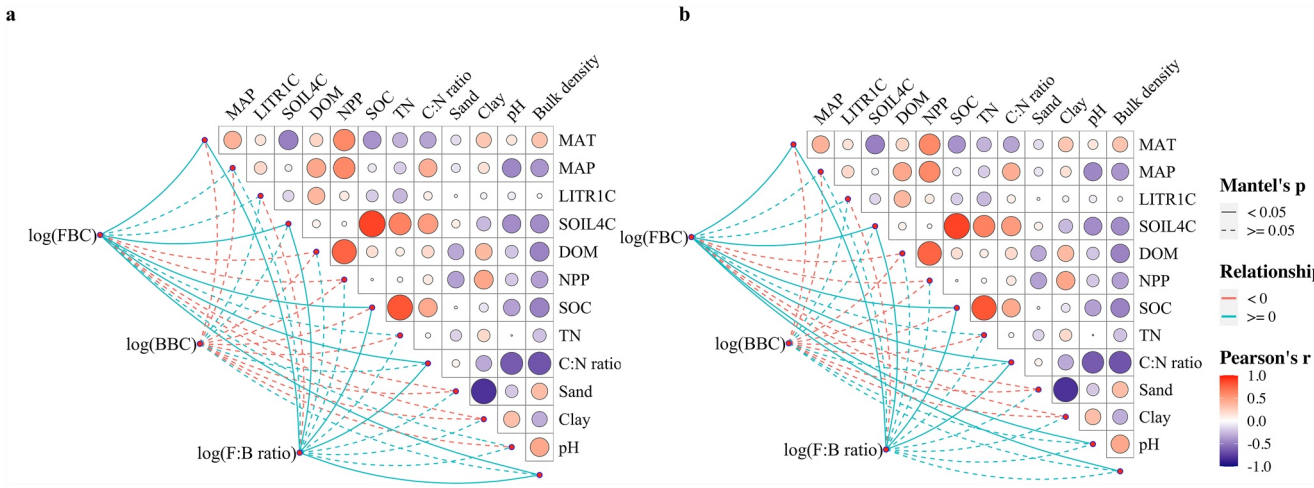


**Figure 2.** Correlations between environmental factors and fungal biomass carbon (FBC), bacterial biomass carbon (BBC), and FBC:BBC (F:B) ratio for (a) observed and (b) simulated data. MAT: mean annual temperature; MAP: mean annual precipitation; LITR1C: labile component of litter, with a turnover time of 20 hr; SOIL4C: the most recalcitrant soil organic matter pool, with a turnover time of 27 years; DOM: dissolved organic matter; NPP: net primary productivity; SOC: soil organic carbon; TN: total nitrogen; C:N ratio, the ratio between SOC and TN. The FBC, BBC, and F:B ratio dissimilarity based on Bray Curtis distance is related to each environmental factor by the Mantel test. Line type indicates the statistical significance ($\alpha = 0.05$), and line color denotes the sign of Pearson's coefficient $r$. For variables included in the analyses, SOC, TN, C:N ratio, pH, Clay, and Sand were observational data at NEON sites, while MAP, MAT, NPP, LITR1C, SOIL4C, and DOM were modeling outputs.

sensitive to anaerobic conditions induced by compacted or inundated soils (Lin et al., 2012). Therefore, changes in bulk density with varying oxygen and water availability can influence fungal biomass.

However, no significant correlations were found between BBC and environmental factors (Figure 2). The lack of environmental controls on BBC indicated the interplay between environmental factors in determining bacterial biomass variations. This can be explained by the synchronous effects of soil ecological factors on bacterial communities. Soil environments are defined by combinations of edaphic and climatic characteristics that microbes need to adapt to in synchrony rather than a single factor (Schimel & Schaeffer, 2012). Our analysis estimating binary interactions between environmental factors using the linear model also confirmed the significant interactions between ST and SM and between TN and Clay on BBC, despite the weak influence of those individual factors on BBC (Table S5 in Supporting Information S1). The combined edaphic effects on bacteria were much stronger than the effects of any single edaphic variable. Such stronger combined effects indicate that the combination of those edaphic factors strengthened the environmental influence on microbial community composition compared with the impact of individual elements.

### 3.4. A Conceptual Framework for the Latitudinal Pattern of Microbial Turnover

Biomass turnover is a crucial biological process for microbes, having important implications on the C cycle (Spohn et al., 2016). Taking advantage of the CLM-Microbe model—a model with soil microbial mechanisms explicitly represented and parametrized, we analyzed the biogeographic pattern and the controls of microbial turnover-related processes (Figure 3). Given that latitude is the most important factor determining fungal and bacterial biomass C turnover and environmental variations are integrated within latitude, we thus analyzed latitudinal trends of fungal and bacterial biomass C turnover and their related processes (Table S6 in Supporting Information S1). Fungal and bacterial biomass C turnover rates quadratically decreased with latitude in the United States (Figures 3a and 3e). This is consistent with our previous work suggesting a positive latitudinal trend in the microbial residence time (He & Xu, 2021; Xu et al., 2017). The positive temperature effects on microbial turnover can explain the decrease in fungal and bacterial biomass C turnover rates with latitude.

Then, we further investigated the latitudinal trends and controls of biomass C turnover-related processes, that is, C assimilation, microbial respiration, and necromass production, for fungi (Figures 3b–3d) and bacteria (Figures 3e–3h). We observed the greatest importance of vegetation NPP in controlling fungal and bacterial C assimilation (Figures 3b and 3f). Vegetation C input as root exudates and litter, components of NPP, is the

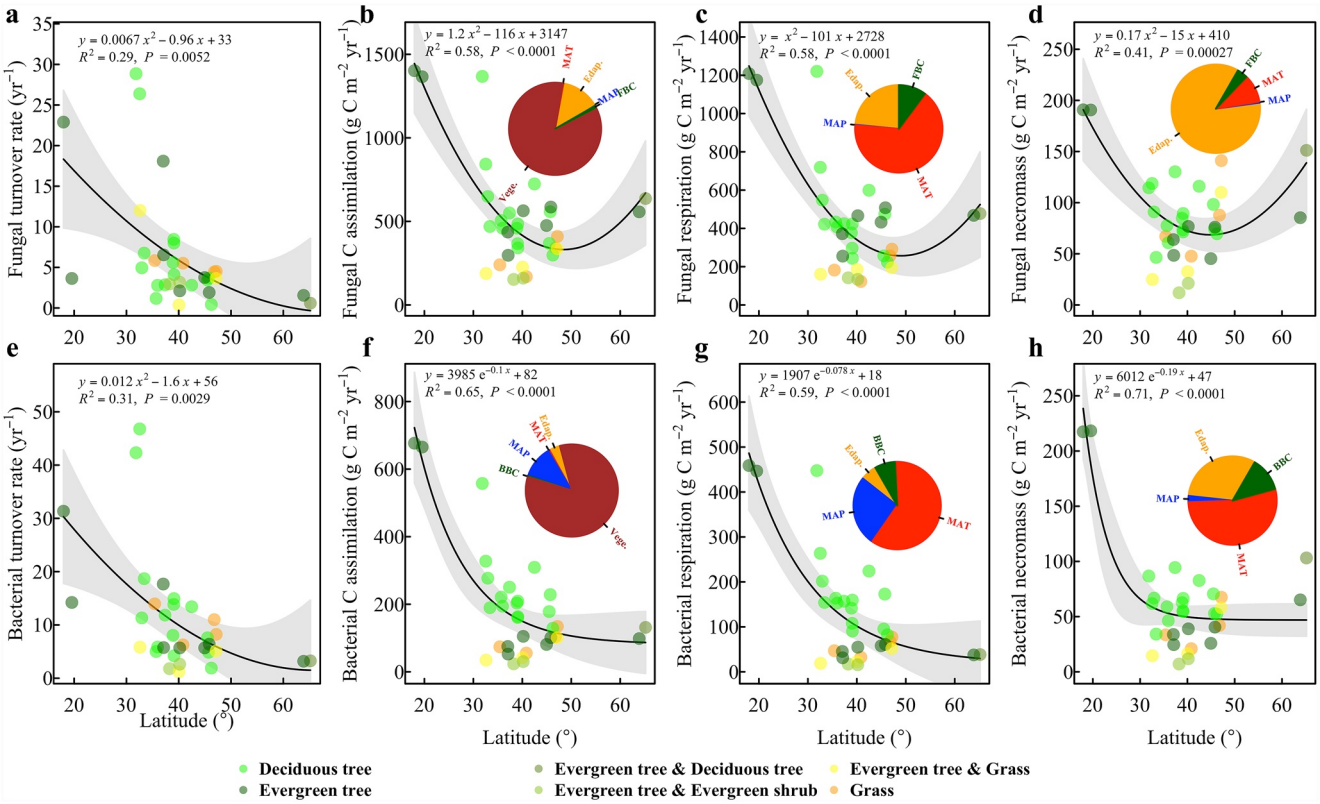


**Figure 3.** Latitudinal patterns of turnover rate, carbon assimilation, microbial respiration, and necromass production for fungi and bacteria; (a) fungal and (e) bacterial turnover rate and fungal (b) carbon assimilation, (c) respiration, and (d) necromass production are quadratic regressions, while trends of bacterial (f) carbon assimilation, (g) respiration, and (h) necromass production are exponential regressions based on the efficiency of regression models. Insets represent the importance of environmental factors on carbon fluxes derived from the XGBoost model. As fungal and bacterial carbon gain and loss decrease along the latitude, those decreases are controlled by varied factors. This shift in fungal and bacterial carbon gain is influenced by vegetation NPP, whereas fungal and bacterial carbon loss as respiration is predominated by MAT. Fungal and bacterial carbon loss as necromass is dominated by different factors, but MAT and edaphic properties are most important for fungal and bacterial carbon loss as necromass. FBC: fungal biomass carbon; BBC: bacterial biomass carbon; MAT: mean annual temperature; MAP: mean annual precipitation; NPP: net primary productivity; Vege: vegetation, that is, net primary productivity in this study; Edap: edaphic properties, which comprises soil organic carbon (SOC), total nitrogen (TN), SOC:TN ratio, sand, silt, clay, pH, and bulk density.

primary C source for soil heterotrophic microbes (Liang & Balser, 2011; Liang et al., 2017). In addition, we found the greatest importance of MAT on fungal and bacterial respiration (Figures 3c and 3g). The prominent role of temperature on microbial respiration has been confirmed by previous studies (Bond-Lamberty & Thomson, 2010; Hamdi et al., 2013; Karhu et al., 2014; Mahecha et al., 2010; Pietikäinen et al., 2005). Microbial respiration shows high sensitivity to temperature variability, following an exponential curve (Mahecha et al., 2010). The decrease in temperature along latitude is thus likely to account for the latitudinal patterns of fungal and bacterial respiration.

In addition, we found the crucial role of MAT and edaphic properties in shaping fungal and bacterial necromass production (Figures 3d and 3h). In line with our findings, Mou et al. (2021) reported the significant role of climatic factors (positive effects of SM and negative effects of ST) and edaphic properties (positive effects of TN) in determining the accumulation of microbial necromass along an elevational gradient in subtropical forests. Ding et al. (2019) confirmed the significant positive role of temperature in the contribution of microbe-derived C to SOC in alpine meadows. However, despite the essential role of MAT and edaphic properties on fungal and bacterial necromass production, MAT and edaphic properties contribute distinctly to the variation of fungal and bacterial necromass production. Specifically, fungal necromass production is dominated by edaphic properties, followed by MAT. While bacterial necromass production is primarily determined by MAT, edaphic properties play a relatively minor role in explaining variations in bacterial necromass production. Necromass is determined by microbial lysis rate which is significantly and positively associated with temperature (He & Xu, 2021). The faster turnover rates of bacteria than of fungi can explain the greater temperature impacts on bacterial necromass production (Rousk & Bååth, 2011). In addition, necromass production is also affected by soil conditions, and

the higher contribution of edaphic properties to fungi necromass production can be attributed to several aspects. First, edaphic properties contributed more to explaining variations in C assimilation of fungal than that of bacteria (Figures 3b and 3f). This may result from the critical contribution of SOM to fungal C assimilation (Table S7 in Supporting Information S1). Second, the hyphae structure extending into the soil matrix contributes to the controlling role of edaphic properties (e.g., silt, pH, and clay) in fungal processes such as necromass production (Wang et al., 2021). Third, the slower turnover rate of fungi weakens the climate effects on necromass production. Fungi have slower turnover rates than bacteria (Figures 3a and 3e). Their differences in turnover rates may indicate weakened stimulating effects of temperature on necromass production for fungi relative to bacteria (Rousk & Bååth, 2011). Lastly, the higher sensitivity of fungi to environmental conditions may also contribute to the higher importance of edaphic impacts on necromass production of fungi relative to bacteria. For example, fungi are more responsive to soil edaphic properties (e.g., SOM quality and quantity, pH, and bulk density) in the United States (Figures S7and S8 in Supporting Information S1).

Despite similar factors controlling microbial C assimilation, respiration, and necromass production for fungi and bacteria, the latitudinal trends of microbial C assimilation, respiration, and necromass production differed between fungi and bacteria (Figures 3b–3d and 3f–3h). The differences in curves of microbial C assimilation and respiration rates between fungi and bacteria may result from the relative contribution of factors in shaping latitudinal trends of fungal and bacterial C assimilation, respiration, and necromass production. Compared with individual variables such as MAT and MAP, edaphic properties include multiple soil physicochemical characteristics and exert complex effects on microbial turnover-related processes (Figure S9 and Table S8 in Supporting Information S1). For example, despite both edaphic properties and MAT being the most important for fungal and bacterial necromass production, we found that necromass production showed an inverse unimodal curve along latitude for fungi but a negative exponential curve for bacteria, with edaphic properties being predominant for fungi and MAT being more dominant for bacteria (Table S7 in Supporting Information S1; Figures 3d and 3h). Similarly, although microbial C assimilation and respiration were predominated by NPP and MAT, respectively, for both fungi and bacteria, MAP played the second most important role in bacteria, while edaphic properties were the second most vital factor for fungi. Such differences in the controlling role of factors and their relative importance resulted in inverse unimodal curves for fungi but the negative exponential curves for bacteria with respect to latitudinal patterns of microbial C assimilation and respiration (Figures 3b, 3c, 3f, and 3g). Therefore, the contributions of environmental factors to the variations in microbial C assimilation, respiration, and necromass production can explain their differences in latitudinal trends for fungi and bacteria.

Taken together, fungal and bacterial biomass C turnover rates quadratically decrease with latitude in the United States (Figure 4). Both fungal and bacterial C assimilation are primarily controlled by vegetation NPP, whereas fungal and bacterial respiration are dominated by MAT. Both fungal and bacterial necromass production were predominately governed by MAT and edaphic properties. However, MAT and edaphic properties contribute distinctly to the variation of fungal and bacterial necromass production. Specifically, fungal necromass production is dominated by edaphic properties, followed by MAT. While bacterial necromass production is primarily determined by MAT, edaphic properties play a relatively minor role in explaining the variation in bacterial necromass production.

### 3.5. Limitations and Prospects

This study investigated the macroecology of fungal and bacterial biomass carbon and turnover rates by integrating observational fungal and bacterial biomass carbon data with the CLM-Microbe model. Findings of this study provide insights into the macroecology of soil microbial communities. Four limitations should be recognized when interesting the results and will be addressed in future work. First, the disproportionate number of data points from climate zones may lead to bias in fungal and bacterial biogeographic patterns. The NEON sampling is based on 20 eco-climate domains, with most in temperate zones. The sampling distribution may introduce bias to the biogeographic patterns identified in this study; a more evenly distributed data set will be used for model validation and testing. Second, biomarkers adopted to indicate fungal and bacterial groups may cause uncertainties in the results. Although biomarkers were identified as indicators of individual microbial groups, some were also found in plants and soil animals. For example, a previous study suggested that fungal PLFAs 18:2ω6, 9c are also common in plants (Zelles, 1997). Third, calibrating the CLM-Microbe model using paired measurements of fungal and bacterial biomass C, respiration rates, turnover rates, necromass production, and

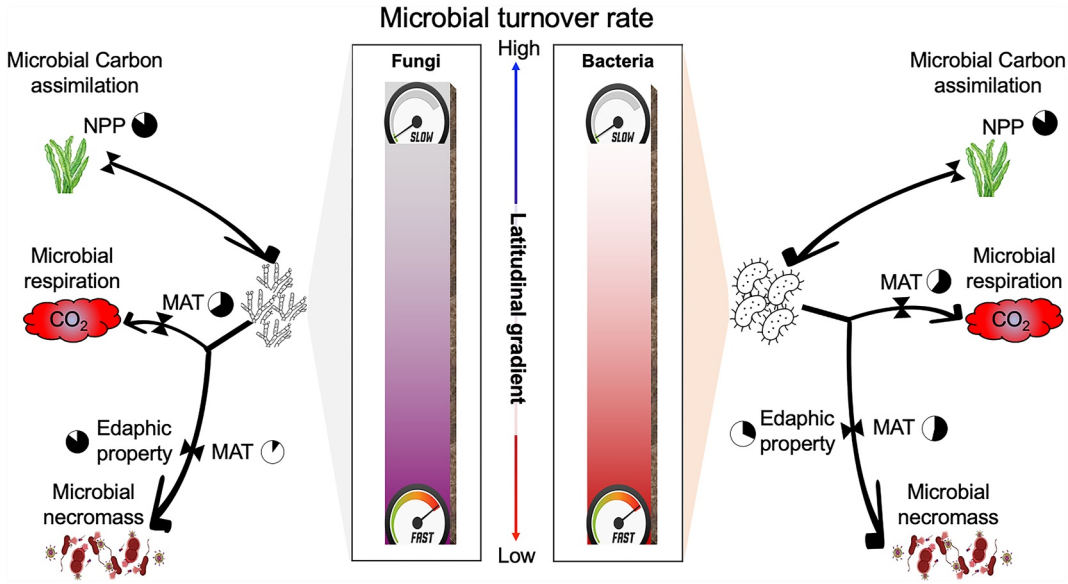


**Figure 4.** Conceptual framework illustrating the differentiation of fungal and bacterial macroecology in topsoil (0–30 cm) in the United States. Pie graphs besides the variables represent the relative importance of various environmental factors on microbial turnover-related processes. MAT: mean annual temperature; MAP: mean annual precipitation; NPP: net primary productivity. The edaphic property includes soil organic carbon (SOC), total nitrogen (TN), SOC: TN ratio, sand, silt, clay, pH, and bulk density. Color bars indicate the latitudinal gradients of fungal and bacterial biomass C turnover rates.

C assimilation rates is needed in constraining the model. Due to data limitations, the CLM-Microbe model was calibrated using fungal and bacterial biomass C provided by NEON (National Ecological Observatory, 2021a) and microbial respiration extracted from the global map (Warner et al., 2019) at the site level. While parameters for the remaining processes are set as default values following the parameterization in our previous work (He, Lipson, et al., 2021), this may introduce uncertainties to the results in this study. Therefore, further research with paired measurements of variables related to fungal and bacterial biomass C dynamics is necessary. Lastly, future improvements are crucial to better represent the microbial community in the CLM-Microbe model. For example, the dormant portion of fungi and bacteria were not considered in the CLM-Microbe model, whereas dormant soil microbes are important for sustaining microbial function and serve as "seed banks" for soil microbial community (Lennon & Jones, 2011).

## 4. Conclusion

The macroecology of microbial biomass C and its turnover is essential for understanding the ecosystem functioning at a regional scale. Our results suggest that fungi exhibit stronger biogeographic patterns than bacteria across the United States. The controls of fungal and bacterial biomass C distribution were different, with FBC significantly associated with climate and edaphic properties and BBC not related to environmental factors. Both fungal and bacterial turnover rates fall quadratically along latitude; however, the latitudinal patterns of their component fluxes (C assimilation, heterotrophic respiration, and necromass production) differed, with quadratic decreases for fungi and reverse exponential trends for bacteria. Microbial C assimilation and respiration were predominately controlled by NPP and MAT, respectively, for both fungi and bacteria. However, necromass production was predominately governed by MAT for bacteria, but edaphic properties dominated that of fungi.

This study represents one of the first efforts to investigate the macroecology of soil fungal and bacterial biomass C and turnover at the continental scale using a data-model integration approach, despite limitations in field observational data and underrepresented microbial mechanisms in the model. These findings provide valuable insights into the biogeographic patterns and underlying mechanisms of fungal and bacterial biomass C and turnover rates. In addition, the responses of fungal and bacterial biomass C and turnover rates to environmental factors shed light on the shifts in the microbial community structure under a changing climate, potentially affecting C cycling and C-climate feedback under future global change scenarios.

## Conflict of Interest

The authors declare no conflicts of interest relevant to this study.

## Data Availability Statement

NEON Soil Microbe Biomass data set (Product ID: DP1.10104.001) is available from https://data.neonscience.org/data-products/DP1.10104.001. The NEON soil physical and chemical properties megapit data set (DP1.10096.001) is available from https://data.neonscience.org/data-products/DP1.00096.001. The CLM-Microbe code is available at the https://doi.org/10.5281/zenodo.7439312. Any other request needs to be directed to the corresponding author.

**Acknowledgments**
This study has been supported by an NSF CAREER project (2145130), an NSF RAPID award (2154746), and the CSU Program for Education & Research in Biotechnology. We acknowledge the operation of the NEON supported by the NSF, which makes the observational data available for this study.

## References

Allison, S. D., & Martiny, J. B. H. (2008). Resistance, resilience, and redundancy in microbial communities. *Proceedings of the National Academy of Sciences of the United States of America*, *105*(1), 11512–11519. https://doi.org/10.1073/pnas.0801925105

Bailey, V. L., Smith, J. L., & Bolton, H. (2002). Fungal-to-bacterial ratios in soils investigated for enhanced C sequestration. *Soil Biology and Biochemistry*, *34*(7), 997–1007. https://doi.org/10.1016/s0038-0717(02)00033-0

Boer, W. d., Folman, L. B., Summerbell, R. C., & Boddy, L. (2005). Living in a fungal world: Impact of fungi on soil bacterial niche development. *FEMS Microbiology Reviews*, *29*(4), 795–811. https://doi.org/10.1016/j.femsre.2004.11.005

Bond-Lamberty, B., & Thomson, A. (2010). Temperature-associated increases in the global soil respiration record. *Nature*, *464*(7288), 579–582. https://doi.org/10.1038/nature08930

Bundt, M., Widmer, F., Pesaro, M., Zeyer, J., & Blaser, P. (2001). Preferential flow paths: Biological "hot spots" in soils. *Soil Biology and Biochemistry*, *33*(6), 729–738. https://doi.org/10.1016/s0038-0717(00)00218-2

Burns, K. N., Bokulich, N. A., Cantu, D., Greenhut, R. F., Kluepfel, D. A., O'Geen, A. T., et al. (2016). Vineyard soil bacterial diversity and composition revealed by 16S rRNA genes: Differentiation by vineyard management. *Soil Biology and Biochemistry*, *103*, 337–348. https://doi.org/10.1016/j.soilbio.2016.09.007

Buyer, J. S., & Sasser, M. (2012). High throughput phospholipid fatty acid analysis of soils. *Applied Soil Ecology*, *61*, 127–130. https://doi.org/10.1016/j.apsoil.2012.06.005

Chapin, F. S., Matson, P. A., & Vitousek, P. (2011). *Principles of terrestrial ecosystem ecology*. Springer Science & Business Media.

Chen, D., Mi, J., Chu, P., Cheng, J., Zhang, L., Pan, Q., et al. (2015). Patterns and drivers of soil microbial communities along a precipitation gradient on the Mongolian Plateau. *Landscape Ecology*, *30*(9), 1669–1682. https://doi.org/10.1007/s10980-014-9996-z

Chen, T., & He, T. (2015). *Xgboost: Extreme gradient boosting*. CRAN. R-Project.

Crowther, T. W., Hoogen, J. V. D., Wan, J., Mayes, M. A., Keiser, A. D., Mo, L., et al. (2019). The global soil community and its influence on biogeochemistry. *Science*, *365*, eaav0550.

Devêvre, O. C., & Horwáth, W. R. (2000). Decomposition of rice straw and microbial carbon use efficiency under different soil temperatures and moistures. *Soil Biology and Biochemistry*, *32*(11–12), 1773–1785. https://doi.org/10.1016/s0038-0717(00)00096-1

Ding, X., Chen, S., Zhang, B., Liang, C., He, H., & Horwath, W. R. (2019). Warming increases microbial residue contribution to soil organic carbon in an alpine meadow. *Soil Biology and Biochemistry*, *135*, 13–19. https://doi.org/10.1016/j.soilbio.2019.04.004

Drenovsky, R. E., Vo, D., Graham, K. J., & Scow, K. M. (2004). Soil water content and organic carbon availability are major determinants of soil microbial community composition. *Microbial Ecology*, *48*(3), 424–430. https://doi.org/10.1007/s00248-003-1063-2

Flato, G. M. (2011). Earth system models: An overview. *Wiley Interdisciplinary Reviews: Climate Change*, *2*(6), 783–800. https://doi.org/10.1002/wcc.148

French, K. E., Tkacz, A., & Turnbull, L. A. (2017). Conversion of grassland to arable decreases microbial diversity and alters community composition. *Applied Soil Ecology*, *110*, 43–52. https://doi.org/10.1016/j.apsoil.2016.10.015

Frostegård, A., & Bååth, E. (1996). The use of phospholipid fatty acid analysis to estimate bacterial and fungal biomass in soil. *Biology and Fertility of Soils*, *22*(1–2), 59–65. https://doi.org/10.1007/bf00384433

Gomez, J. D., Denef, K., Stewart, C. E., Zheng, J., & Cotrufo, M. F. (2014). Biochar addition rate influences soil microbial abundance and activity in temperate soils. *European Journal of Soil Science*, *65*(1), 28–39. https://doi.org/10.1111/ejss.12097

Gomez-Casanovas, N., Matamala, R., Cook, D. R., & Gonzalez-Meler, M. A. (2012). Net ecosystem exchange modifies the relationship between the autotrophic and heterotrophic components of soil respiration with abiotic factors in prairie grasslands. *Global Change Biology*, *18*(8), 2532–2545. https://doi.org/10.1111/j.1365-2486.2012.02721.x

Gu, L., Post, W. M., & King, A. W. (2004). Fast labile carbon turnover obscures sensitivity of heterotrophic respiration from soil to temperature: A model analysis. *Global Biogeochemical Cycles*, *18*(1). https://doi.org/10.1029/2003gb002119

Haefner, J. W. (2005). *Modeling biological systems-principles and applications*. Springer.

Hamdi, S., Moyano, F., Sall, S., Bernoux, M., & Chevallier, T. (2013). Synthesis analysis of the temperature sensitivity of soil respiration from laboratory studies in relation to incubation methods and soil conditions. *Soil Biology and Biochemistry*, *58*, 115–126. https://doi.org/10.1016/j.soilbio.2012.11.012

Hargrove, W. W., & Hoffman, F. M. (2004). Potential of multivariate quantitative methods for delineation and visualization of ecoregions. *Environmental Management*, *34*(S1), S39–S60. https://doi.org/10.1007/s00267-003-1084-0

Harper, C. W., Blair, J. M., Fay, P. A., Knapp, A. K., & Carlisle, J. D. (2005). Increased rainfall variability and reduced rainfall amount decreases soil $CO_2$ flux in a grassland ecosystem. *Global Change Biology*, *11*(2), 322–334. https://doi.org/10.1111/j.1365-2486.2005.00899.x

He, L., Lai, C.-T., Mayes, M. A., Murayama, S., & Xu, X. (2021). Microbial seasonality promotes soil respiratory carbon emission in natural ecosystems: A modeling study. *Global Change Biology*, *27*(13), 3035–3051. https://doi.org/10.1111/gcb.15627

He, L., Lipson, D. A., Rodrigues, J. L. M., Mayes, M., Björk, R. G., Glaser, B., et al. (2021). Dynamics of fungal and bacterial biomass carbon in natural ecosystems: Site-level applications of the CLM-microbe model. *Journal of Advances in Modeling Earth Systems*, *13*, e2020MS002283. https://doi.org/10.1029/2020MS002283

He, L., Rodrigues, J. L. M., Soudzilovskaia, N. A., Barceló, M., Olsson, P. a. A., Song, C., et al. (2020). Global biogeography of fungal and bacterial biomass carbon in topsoil. *Soil Biology and Biochemistry*, *151*, 108024. https://doi.org/10.1016/j.soilbio.2020.108024

He, L., & Xu, X. (2021). Mapping soil microbial residence time at the global scale. *Global Change Biology*, *27*(24), 6484–6497. https://doi.org/10.1111/gcb.15864

Högberg, M. N., Högberg, P., & Myrold, D. D. (2007). Is microbial community composition in boreal forest soils determined by pH, C-to-N ratio, the trees, or all three? *Oecologia*, *150*(4), 590–601. https://doi.org/10.1007/s00442-006-0562-5

Huang, H. (2021). *linkET: Everything is linkable*. CRAN. R-Project.

Jobbágy, E. G., & Jackson, R. B. (2000). The vertical distribution of soil organic carbon and its relation to climate and vegetation. *Ecological Applications*, *10*(2), 423–436. https://doi.org/10.1890/1051-0761(2000)010[0423:tvdoso]2.0.co;2

Joergensen, R. G., Brookes, P. C., & Jenkinson, D. S. (1990). Survival of the soil microbial biomass at elevated temperatures. *Soil Biology and Biochemistry*, *22*(8), 1129–1136. https://doi.org/10.1016/0038-0717(90)90039-3

Kaisermann, A., Maron, P. A., Beaumelle, L., & Lata, J. C. (2015). Fungal communities are more sensitive indicators to non-extreme soil moisture variations than bacterial communities. *Applied Soil Ecology*, *86*, 158–164. https://doi.org/10.1016/j.apsoil.2014.10.009

Kampe, T. U., Johnson, B. R., Kuester, M. A., & Keller, M. (2010). NEON: The first continental-scale ecological observatory with airborne remote sensing of vegetation canopy biochemistry and structure. *Journal of Applied Remote Sensing*, *4*(1), 043510. https://doi.org/10.1117/1.3361375

Kao, R. H., Gibson, C. M., Gallery, R. E., Meier, C. L., Barnett, D. T., Docherty, K. M., et al. (2012). NEON terrestrial field observations: Designing continental-scale, standardized sampling. *Ecosphere*, *3*(12), 1–17. https://doi.org/10.1890/es12-00196.1

Karhu, K., Auffret, M. D., Dungait, J. A. J., Hopkins, D. W., Prosser, J. I., Singh, B. K., et al. (2014). Temperature sensitivity of soil respiration rates enhanced by microbial community response. *Nature*, *513*(7516), 81–84. https://doi.org/10.1038/nature13604

Keller, M., Schimel, D. S., Hargrove, W. W., & Hoffman, F. M. (2008). *A continental strategy for the national ecological observatory network* (pp. 282–284). The Ecological Society of America.

Kemmitt, S. J., Wright, D., Goulding, K. W. T., & Jones, D. L. (2006). pH regulation of carbon and nitrogen dynamics in two agricultural soils. *Soil Biology and Biochemistry*, *38*(5), 898–911. https://doi.org/10.1016/j.soilbio.2005.08.006

Klamer, M., & Bååth, E. (2004). Estimation of conversion factors for fungal biomass determination in compost using ergosterol and PLFA 18: 2$ømega$6, 9. *Soil Biology and Biochemistry*, *36*(1), 57–65. https://doi.org/10.1016/j.soilbio.2003.08.019

Koven, C. D., Riley, W. J., Subin, Z. M., Tang, J. Y., Torn, M. S., Collins, W. D., et al. (2013). The effect of vertically resolved soil biogeochemistry and alternate soil C and N models on C dynamics of CLM4. *Biogeosciences*, *10*(11), 7109–7131. https://doi.org/10.5194/bg-10-7109-2013

Lennon, J. T., & Jones, S. E. (2011). Microbial seed banks: The ecological and evolutionary implications of dormancy. *Nature Reviews Microbiology*, *9*(2), 119–130. https://doi.org/10.1038/nrmicro2504

Liang, C., & Balser, T. C. (2011). Microbial production of recalcitrant organic matter in global soils: Implications for productivity and climate policy. *Nature Reviews Microbiology*, *9*(1), 75. https://doi.org/10.1038/nrmicro2386-c1

Liang, C., Schimel, J. P., & Jastrow, J. D. (2017). The importance of anabolism in microbial control over soil carbon storage. *Nature Microbiology*, *2*(8), 1–6. https://doi.org/10.1038/nmicrobiol.2017.105

Lin, X., Green, S., Tfaily, M. M., Prakash, O., Konstantinidis, K. T., Corbett, J. E., et al. (2012). Microbial community structure and activity linked to contrasting biogeochemical gradients in bog and fen environments of the Glacial Lake Agassiz Peatland. *Applied and Environmental Microbiology*, *78*(19), 7023–7031. https://doi.org/10.1128/aem.01750-12

Lipson, D. A., Schmidt, S. K., & Monson, R. K. (1999). Links between microbial population dynamics and nitrogen availability in an alpine ecosystem. *Ecology*, *80*(5), 1623–1631. https://doi.org/10.1890/0012-9658(1999)080[1623:lbmpda]2.0.co;2

Mahecha, M. D., Reichstein, M., Carvalhais, N., Lasslop, G., Lange, H., Seneviratne, S. I., et al. (2010). Global convergence in the temperature sensitivity of respiration at ecosystem level. *Science*, *329*(5993), 838–840. https://doi.org/10.1126/science.1189587

Manzoni, S., Schimel, J. P., & Porporato, A. (2012). Responses of soil microbial communities to water stress: Results from a meta-analysis. *Ecology*, *93*(4), 930–938. https://doi.org/10.1890/11-0026.1

Martiny, J. B. H., Bohannan, B. J. M., Brown, J. H., Colwell, R. K., Fuhrman, J. A., Green, J. L., et al. (2006). Microbial biogeography: Putting microorganisms on the map. *Nature Reviews Microbiology*, *4*(2), 102–112. https://doi.org/10.1038/nrmicro1341

Marumoto, T., Anderson, J. P. E., & Domsch, K. H. (1982). Mineralization of nutrients from soil microbial biomass. *Soil Biology and Biochemistry*, *14*(5), 469–475. https://doi.org/10.1016/0038-0717(82)90106-7

Mei, W., Yu, G., Lai, J., Rao, Q., & Umezawa, Y. (2018). basicTrendline: Add Trendline and confidence interval of basic regression models to plot, R package version 2.0.3. Retrieved from https://CRAN.R-project.org/package=basicTrendline

Metzger, S., Ayres, E., Durden, D., Florian, C., Lee, R., Lunch, C., et al. (2019). From NEON field sites to data portal: A community resource for surface–atmosphere research comes online. *Bulletin of the American Meteorological Society*, *100*(11), 2305–2325. https://doi.org/10.1175/bams-d-17-0307.1

Moeys, J. (2018). *The soil texture wizard: R functions for plotting, classifying, transforming and exploring soil texture data*. CRAN. R-Project.

Mou, Z., Kuang, L., He, L., Zhang, J., Zhang, X., Hui, D., et al. (2021). Climatic and edaphic controls over the elevational pattern of microbial necromass in subtropical forests. *CATENA*, *207*, 105707. https://doi.org/10.1016/j.catena.2021.105707

National Ecological Observatory, N. (2021a). *Soil microbe biomass (DP1.10104.001)*. National Ecological Observatory Network (NEON).

National Ecological Observatory, N. (2021b). *Soil physical and chemical properties, Megapit (DP1.00096.001)*. National Ecological Observatory Network (NEON).

Phillips, L. A., Ward, V., & Jones, M. D. (2014). Ectomycorrhizal fungi contribute to soil organic matter cycling in sub-boreal forests. *The ISME Journal*, *8*(3), 699–713. https://doi.org/10.1038/ismej.2013.195

Pietikäinen, J., Pettersson, M., & Bååth, E. (2005). Comparison of temperature effects on soil respiration and bacterial and fungal growth rates. *FEMS Microbiology Ecology*, *52*(1), 49–58. https://doi.org/10.1016/j.femsec.2004.10.002

Rousk, J., & Bååth, E. (2007a). Fungal and bacterial growth in soil with plant materials of different C/N ratios. *FEMS Microbiology Ecology*, *62*(3), 258–267. https://doi.org/10.1111/j.1574-6941.2007.00398.x

Rousk, J., & Bååth, E. (2011). Growth of saprotrophic fungi and bacteria in soil. *FEMS Microbiology Ecology*, *78*(1), 17–30. https://doi.org/10.1111/j.1574-6941.2011.01106.x

Rousk, J., Bååth, E., Brookes, P. C., Lauber, C. L., Lozupone, C., Caporaso, J. G., et al. (2010a). Soil bacterial and fungal communities across a pH gradient in an arable soil. *The ISME Journal*, *4*(10), 1340–1351. https://doi.org/10.1038/ismej.2010.58

Rousk, J., Brookes, P. C., & Bååth, E. (2009). Contrasting soil pH effects on fungal and bacterial growth suggest functional redundancy in carbon mineralization. *Applied and Environmental Microbiology*, *75*(6), 1589–1596. https://doi.org/10.1128/aem.02775-08

Rousk, J., Brookes, P. C., & Bååth, E. (2010b). Investigating the mechanisms for the opposing pH relationships of fungal and bacterial growth in soil. *Soil Biology and Biochemistry*, *42*(6), 926–934. https://doi.org/10.1016/j.soilbio.2010.02.009

Schimel, J., & Schaeffer, S. M. (2012). Microbial control over carbon cycling in soil. *Frontiers in Microbiology*, *3*. https://doi.org/10.3389/fmicb.2012.00348

Schnürer, J., Clarholm, M., & Rosswall, T. (1985). Microbial biomass and activity in an agricultural soil with different organic matter contents. *Soil Biology and Biochemistry*, *17*(5), 611–618. https://doi.org/10.1016/0038-0717(85)90036-7

Sinsabaugh, R. L., Manzoni, S., Moorhead, D. L., & Richter, A. (2013). Carbon use efficiency of microbial communities: Stoichiometry, methodology and modelling. *Ecology Letters*, *16*(7), 930–939. https://doi.org/10.1111/ele.12113

Sokol, N. W., Slessarev, E., Marschmann, G. L., Nicolas, A., Blazewicz, S. J., Brodie, E. L., et al. (2022). Life and death in the soil microbiome: How ecological processes influence biogeochemistry. *Nature Reviews Microbiology*, *20*(7), 1–16. https://doi.org/10.1038/s41579-022-00695-z

Sparling, G. P. (1997). Soil microbial biomass, activity and nutrient cycling as indicators of soil health. Biological indicators of soil health (pp. 97–119).

Spohn, M., Klaus, K., Wanek, W., & Richter, A. (2016). Microbial carbon use efficiency and biomass turnover times depending on soil depth–Implications for carbon cycling. *Soil Biology and Biochemistry*, *96*, 74–81. https://doi.org/10.1016/j.soilbio.2016.01.016

Talbot, J. M., Bruns, T. D., Smith, D. P., Branco, S., Glassman, S. I., Erlandson, S., et al. (2013). Independent roles of ectomycorrhizal and saprotrophic communities in soil organic matter decomposition. *Soil Biology and Biochemistry*, *57*, 282–291. https://doi.org/10.1016/j.soilbio.2012.10.004

Thornton, P. E., Lamarque, J. F., Rosenbloom, N. A., & Mahowald, N. M. (2007). Influence of carbon-nitrogen cycle coupling on land model response to $CO_2$ fertilization and climate variability. *Global Biogeochemical Cycles*, *21*(4), GB4018. https://doi.org/10.1029/2006gb002868

Thornton, P. E., & Rosenbloom, N. A. (2005). Ecosystem model spin-up: Estimating steady state conditions in a coupled terrestrial carbon and nitrogen cycle model. *Ecological Modelling*, *189*(1–2), 25–48. https://doi.org/10.1016/j.ecolmodel.2005.04.008

Van Der Heijden, M. G. A., Bardgett, R. D., & Van Straalen, N. M. (2008). The unseen majority: Soil microbes as drivers of plant diversity and productivity in terrestrial ecosystems. *Ecology Letters*, *11*(3), 296–310. https://doi.org/10.1111/j.1461-0248.2007.01139.x

Waldrop, M. P., Holloway, J. M., Smith, D. B., Goldhaber, M. B., Drenovsky, R. E., Scow, K. M., et al. (2017). The interacting roles of climate, soils, and plant production on soil microbial communities at a continental scale. *Ecology*, *98*(7), 1957–1967. https://doi.org/10.1002/ecy.1883

Wang, B., An, S., Liang, C., Liu, Y., & Kuzyakov, Y. (2021). Microbial necromass as the source of soil organic carbon in global ecosystems. *Soil Biology and Biochemistry*, *162*, 108422. https://doi.org/10.1016/j.soilbio.2021.108422

Wang, Y., Yuan, F., Yuan, F., Gu, B., Hahn, M. S., Torn, M. S., et al. (2019). Mechanistic modeling of microtopographic impacts on $CO_2$ and $CH_4$ Fluxes in an Alaskan tundra ecosystem using the CLM-Microbe model. *Journal of Advances in Modeling Earth Systems*, *11*(12), 17–4304. https://doi.org/10.1029/2019ms001771

Warner, D. L., Bond-Lamberty, B. P., Jian, J., Stell, E., & Vargas, R. (2019). *Global gridded 1-km annual soil respiration and uncertainty derived from SRDB V3*. ORNL Distributed Active Archive Center.

Wickham, H., & Chang, W. (2016). ggplot2: Create elegant data visualisations using the grammar of graphics, R package version 2.1. Retrieved from https://CRAN.R-project.org/package=ggplot2

Willers, C., Jansen van Rensburg, P. J., & Claassens, S. (2015). Phospholipid fatty acid profiling of microbial communities–a review of interpretations and recent applications. *Journal of Applied Microbiology*, *119*(5), 1207–1218. https://doi.org/10.1111/jam.12902

Xu, X., Elias, D. A., Graham, D. E., Phelps, T. J., Carroll, S. L., Wullschleger, S. D., & Thornton, P. E. (2015). A microbial functional group-based module for simulating methane production and consumption: Application to an incubated permafrost soil. *Journal of Geophysical Research: Biogeosciences*, *120*(7), 1315–1333. https://doi.org/10.1002/2015jg002935

Xu, X., He, L., & Wang, Y. (2022). CLM-Microbe v1.0 [Software]. Zenodo. https://doi.org/10.5281/zenodo.7439312

Xu, X., Schimel, J. P., Janssens, I. A., Song, X., Song, C., Yu, G., et al. (2017). Global pattern and controls of soil microbial metabolic quotient. *Ecological Monographs*, *87*(3), 429–441. https://doi.org/10.1002/ecm.1258

Xu, X., Schimel, J. P., Thornton, P. E., Song, X., Yuan, F., & Goswami, S. (2014). Substrate and environmental controls on microbial assimilation of soil organic carbon: A framework for earth system models. *Ecology Letters*, *17*(5), 547–555. https://doi.org/10.1111/ele.12254

Xu, X., Thornton, P. E., & Post, W. M. (2013). A global analysis of soil microbial biomass carbon, nitrogen and phosphorus in terrestrial ecosystems. *Global Ecology and Biogeography*, *22*(6), 737–749. https://doi.org/10.1111/geb.12029

Xu, X., Wang, N., Lipson, D., Sinsabaugh, R., Schimel, J., He, L., et al. (2020). Microbial macroecology: In search of mechanisms governing microbial biogeographic patterns. *Global Ecology and Biogeography*, *29*(11), 1870–1886. https://doi.org/10.1111/geb.13162

Yu, K., van den Hoogen, J., Wang, Z., Averill, C., Routh, D., Smith, G. R., et al. (2022). The biogeography of relative abundance of soil fungi versus bacteria in surface topsoil. *Earth System Science Data*, *14*(9), 4339–4350. https://doi.org/10.5194/essd-14-4339-2022

Zelles, L. (1997). Phospholipid fatty acid profiles in selected members of soil microbial communities. *Chemosphere*, *35*(1–2), 275–294. https://doi.org/10.1016/s0045-6535(97)00155-0

Zelles, L. (1999). Fatty acid patterns of phospholipids and lipopolysaccharides in the characterisation of microbial communities in soil: A review. *Biology and Fertility of Soils*, *29*(2), 111–129. https://doi.org/10.1007/s003740050533

Zhang, Q., Lei, H.-M., & Yang, D.-W. (2013). Seasonal variations in soil respiration, heterotrophic respiration and autotrophic respiration of a wheat and maize rotation cropland in the North China Plain. *Agricultural and Forest Meteorology*, *180*, 34–43. https://doi.org/10.1016/j.agrformet.2013.04.028

Zhang, X., Dai, G., Ma, T., Liu, N., Hu, H., Ma, W., et al. (2020). Links between microbial biomass and necromass components in the top-and subsoils of temperate grasslands along an aridity gradient. *Geoderma*, *379*, 114623. https://doi.org/10.1016/j.geoderma.2020.114623

Zhang, Y., Zheng, N., Wang, J., Yao, H., Qiu, Q., & Chapman, S. J. (2019). High turnover rate of free phospholipids in soil confirms the classic hypothesis of PLFA methodology. *Soil Biology and Biochemistry*, *135*, 323–330. https://doi.org/10.1016/j.soilbio.2019.05.023

Zhou, Z., Wang, C., Zheng, M., Jiang, L., & Luo, Y. (2017). Patterns and mechanisms of responses by soil microbial communities to nitrogen addition. *Soil Biology and Biochemistry*, *115*, 433–441. https://doi.org/10.1016/j.soilbio.2017.09.015

## References From the Supporting Information

Bahram, M., Hildebrand, F., Forslund, S. K., Anderson, J. L., Soudzilovskaia, N. A., Bodegom, P. M., et al. (2018). Structure and function of the global topsoil microbiome. *Nature*, *560*(7717), 233–237. https://doi.org/10.1038/s41586-018-0386-6

Bell, C. W., Acosta-Martinez, V., McIntyre, N. E., Cox, S., Tissue, D. T., & Zak, J. C. (2009). Linking microbial community structure and function to seasonal differences in soil moisture and temperature in a Chihuahuan desert grassland. *Microbial Ecology*, *58*(4), 827–842. https://doi.org/10.1007/s00248-009-9529-5

Cherrier, J., Bauer, J., & Druffel, E. (1996). Utilization and turnover of labile dissolved organic matter by bacterial heterotrophs in eastern North Pacific surface waters. *Marine Ecology Progress Series*, *139*, 267–279. https://doi.org/10.3354/meps139267

Cleveland, C. C., Townsend, A. R., & Schmidt, S. K. (2002). Phosphorus limitation of microbial processes in moist tropical forests: Evidence from short-term laboratory incubations and field studies. *Ecosystems*, *5*(7), 0680–0691. https://doi.org/10.1007/s10021-002-0202-9

Demoling, F., Nilsson, L. O., & Bååth, E. (2008). Bacterial and fungal response to nitrogen fertilization in three coniferous forest soils. *Soil Biology and Biochemistry*, *40*(2), 370–379. https://doi.org/10.1016/j.soilbio.2007.08.019

Díaz-Raviña, M., Acea, M. J., & Carballas, T. (1995). Seasonal changes in microbial biomass and nutrient flush in forest soils. *Biology and Fertility of Soils*, *19*(2–3), 220–226. https://doi.org/10.1007/bf00336163

Eskelinen, A., Stark, S., & Männistö, M. (2009). Links between plant community composition, soil organic matter quality and microbial communities in contrasting tundra habitats. *Oecologia*, *161*(1), 113–123. https://doi.org/10.1007/s00442-009-1362-5

Frey, S. D., Elliott, E. T., & Paustian, K. (1999). Bacterial and fungal abundance and biomass in conventional and no-tillage agroecosystems along two climatic gradients. *Soil Biology and Biochemistry*, *31*(4), 573–585. https://doi.org/10.1016/s0038-0717(98)00161-8

Frey-Klett, P., Burlinson, P., Deveau, A., Barret, M., Tarkka, M., & Sarniguet, A. (2011). Bacterial-fungal interactions: Hyphens between agricultural, clinical, environmental, and food microbiologists. *Microbiology and Molecular Biology Reviews*, *75*(4), 583–609. https://doi.org/10.1128/mmbr.00020-11

Gommers, P. J. F., Schie, B. J. v., Dijken, J. P. v., & Kuenen, J. G. (1988). Biochemical limits to microbial growth yields: An analysis of mixed substrate utilization. *Biotechnology and Bioengineering*, *32*(1), 86–94. https://doi.org/10.1002/bit.260320112

Kirchman, D. L., Suzuki, Y., Garside, C., & Ducklow, H. W. (1991). High turnover rates of dissolved organic carbon during a spring phytoplankton bloom. *Nature*, *352*(6336), 612–614. https://doi.org/10.1038/352612a0

Lipson, D. A., Schadt, C. W., & Schmidt, S. K. (2002). Changes in soil microbial community structure and function in an alpine dry meadow following spring snow melt. *Microbial Ecology*, *43*(3), 307–314. https://doi.org/10.1007/s00248-001-1057-x

Liu, L., & Greaver, T. L. (2010). A global perspective on belowground carbon dynamics under nitrogen enrichment. *Ecology Letters*, *13*(7), 819–828. https://doi.org/10.1111/j.1461-0248.2010.01482.x

McKane, R. B., Johnson, L. C., Shaver, G. R., Nadelhoffer, K. J., Rastetter, E. B., Fry, B., et al. (2002). Resource-based niches provide a basis for plant species diversity and dominance in arctic tundra. *Nature*, *415*(6867), 68–71. https://doi.org/10.1038/415068a

Mille-Lindblom, C., Fischer, H., & Tranvik, L. J. (2006). Antagonism between bacteria and fungi: Substrate competition and a possible tradeoff between fungal growth and tolerance towards bacteria. *Oikos*, *113*(2), 233–242. https://doi.org/10.1111/j.2006.0030-1299.14337.x

Moore, J. C., McCann, K., & de Ruiter, P. C. (2005). Modeling trophic pathways, nutrient cycling, and dynamic stability in soils. *Pedobiologia*, *49*(6), 499–510. https://doi.org/10.1016/j.pedobi.2005.05.008

Rousk, J., & Bååth, E. (2007b). Fungal biomass production and turnover in soil estimated using the acetate-in-ergosterol technique. *Soil Biology and Biochemistry*, *39*(8), 2173–2177. https://doi.org/10.1016/j.soilbio.2007.03.023

Schippers, A., Neretin, L. N., Kallmeyer, J., Ferdelman, T. G., Cragg, B. A., John Parkes, R., & Jørgensen, B. B. (2005). Prokaryotic cells of the deep sub-seafloor biosphere identified as living bacteria. *Nature*, *433*(7028), 861–864. https://doi.org/10.1038/nature03302

Sinsabaugh, R. L., Turner, B. L., Talbot, J. M., Waring, B. G., Powers, J. S., Kuske, C. R., et al. (2016). Stoichiometry of microbial carbon use efficiency in soils. *Ecological Monographs*, *86*(2), 172–189. https://doi.org/10.1890/15-2110.1

Sistla, S. A., Asao, S., & Schimel, J. P. (2012). Detecting microbial N-limitation in tussock tundra soil: Implications for arctic soil organic carbon cycling. *Soil Biology and Biochemistry*, *55*, 78–84. https://doi.org/10.1016/j.soilbio.2012.06.010

Strickland, M. S., & Rousk, J. (2010). Considering fungal: Bacterial dominance in soils–methods, controls, and ecosystem implications. *Soil Biology and Biochemistry*, *42*(9), 1385–1395. https://doi.org/10.1016/j.soilbio.2010.05.007

Wallander, H. a., Göransson, H., & Rosengren, U. (2004). Production, standing biomass and natural abundance of 15 N and 13 C in ectomycorrhizal mycelia collected at different soil depths in two forest types. *Oecologia*, *139*(1), 89–97. https://doi.org/10.1007/s00442-003-1477-z

Wheeler, P. A., Gosselin, M., Sherr, E., Thibaultc, D., Kirchman, D. L., Benner, R., & Whitledge, T. E. (1996). Active cycling of organic carbon in the central Arctic Ocean. *Nature*, *380*(6576), 697–699. https://doi.org/10.1038/380697a0